of poles and optic axis, the center of the plot being the normal to the thin section. All projections were then normalized by rotating the optic axis into the center. The new positions of the poles — resulting from this rotation — are indicated by circles. This standard projection allows the identification of the poles of planar elements with crystallographic planes. By definition a pole was assumed to coincide with a crystallographic plane if the angle between measured and ideal plane differed less than 5°. This allowance corresponds to the accuracy of universal stage measurements. This method allows a more precise identification of planar

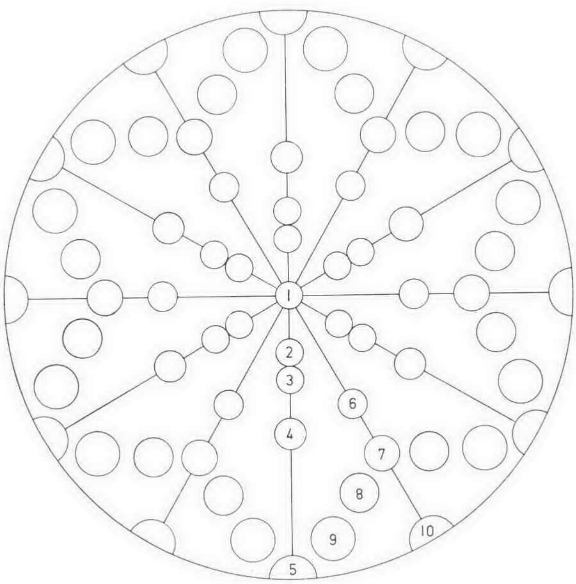

Fig. 10. Crystallographic orientation of the observed planar structures. Angles between poles of planes and optic axis:
1. (0001): 0°
2. (10$\bar{1}$3): 22°56'
3. (10$\bar{1}$2): 32°25'
4. (10$\bar{1}$1): 51°47'
5. (10$\bar{1}$0): 90°
6. (11$\bar{2}$2): 47°43'
7. (11$\bar{2}$1): 65°33'
8. (21$\bar{3}$1): 73°25'
9. (51$\bar{6}$1): 81°57'
10. (11$\bar{2}$0): 90°

structures with low index planes as compared to measurements of their angle to the optic axis alone, the method commonly used by various authors. The orientation of all planar structures investigated is shown in Fig. 10. The diameters of the circles correspond to the 5° accuracy of the measurements.

Approximately 50 grains have been measured per each thin section. On the average 3 to 10 different sets of planar structures per grain were observed with a maximum of 18 sets for a single grain.

Qualitative frequencies concerning the various types of deformation structures are given in Table 2. Quantitative frequencies of all features combined are listed in Tables 3 and 4 and illustrated in Figs. 10 and 11.

The following parameters have been reduced from the microscopical data:

q_{hkil} = actual number of symmetrically equivalent deformation planes $\{hkil\}$ observed in n quartz grains.

p_{hkil} = maximum number of symmetrically equivalent planes $\{hkil\}$ potentially observable in n quartz grains, accounting for the limitations of grain orientation and blind circle.

Q = total number of all sets of planar structures observed in n quartz grains.

Table 2. *Qualitative frequencies of planar deformation structures in quartz of the investigated rock samples*

No. of rock sample	Planar structures					Irregular fractures
	decorated planar elements	non-decorated planar elements	homogeneous lamellae	filled lamellae	planar fractures	
B 10	some	few	—	—	some	very many
B 51	many	few	very few	—	some	very many
S 289	—	many	—	very many	some	many
B 36	very many	few	many	—	some	many
B 151	many	many	some	—	some	some
B 1	many	many	few	—	some	many
S 350	many	many	some	—	some	some
S 349	many	very many	some	—	some	some
B 7	—	very many	very few	—	some	few
B 9	—	very many	very few	—	some	some

Table 3. *Relative frequencies f_{hkil} (%) of planar structures in quartz from Ries rocks*

Sample No.	B 10	B 51	S 289	B 36	B 151	B 1	S 350	S 349	B 7	B 9
$\{0001\}$	21	20	0	22	2	57	33	2	9	13
$\{10\bar{1}3\}$	44	53	60	52	66	53	68	55	51	63
$\{10\bar{1}2\}$	0.5	1	31	31	32	34	59	45	52	49
$\{10\bar{1}1\}$	3	6	18	19	30	33	40	26	6	27
$\{11\bar{2}2\}$	1	3	3	6	5	8	1	6	4	5
$\{11\bar{2}1\}$	0.3	1	5	3	4	7	3	8	6	4
$\{21\bar{3}1\}$	1	2	4	6	7	9	7	7	6	7
$\{51\bar{6}1\}$	1	2	4	3	4	5	2	5	3	4
$\{10\bar{1}0\}$ $\{11\bar{2}0\}$	1	2	2	4	6	12	6	8	4	8
Sets per grain	2.8	4	6.7	7.3	9	11	10	8.8	7.6	9.2

Table 4. *Absolute frequencies F_{hkil} (%) of planar structures in quartz from Ries rocks*

Sample No:	B 10	B 51	S 289	B 36	B 151	B 1	S 350	S 349	B 7	B 9
$\{0001\}$	6	5	0	3	0.2	5	3	0.2	1	1
$\{10\bar{1}3\}$	75	70	44	38	42	29	34	33	38	37
$\{10\bar{1}2\}$	1	2	22	22	19	17	30	25	36	27
$\{10\bar{1}1\}$	6	7	13	12	16	15	20	14	4	14
$\{11\bar{2}2\}$	2	4	2	4	3	4	0.3	3	3	2
$\{11\bar{2}1\}$	0.5	1	4	2	2	3	1	4	3	2
$\{21\bar{3}1\}$	2	3	6	8	7	8	7	6	7	8
$\{51\bar{6}1\}$	4	4	5	4	4	5	2	5	4	4
$\{10\bar{1}0\}$ $\{11\bar{2}0\}$	2	2	2	3	3	5	3	4	2	4
Not identified:	1.4	3	3	4	4	11	0.6	6	3	1.3